

# A Comparison of Avalanche Photodiode and Photomultiplier Tube Detectors for Flow Cytometry

William G. Lawrence<sup>a</sup>, Gyula Varadi<sup>a</sup>, Gerald. Entine<sup>a</sup>, Edward Podniesinski<sup>b</sup>, and Paul K. Wallace<sup>b</sup>

<sup>a</sup>Radiation Monitoring Devices Inc., 44 Hunt St., Watertown MA 02472;

<sup>b</sup>Roswell Park Cancer Institute, Elm and Carlton Streets, Buffalo NY 14263

## ABSTRACT

Commercial flow cytometers use photomultiplier tubes (PMTs) for fluorescence detection. These detectors have high linear gain and broad dynamic range, but have limited sensitivity in the red and near infrared spectral regions. We present a comparison of avalanche photodiodes (APDs) and PMTs as detectors in flow cytometry instruments, and demonstrate improved sensitivity and resolution in the red and near infrared spectral regions using the APD. The relative performance of the PMT and APD were evaluated by simultaneously measuring the mean fluorescence intensity and coefficient of variation for emission from light emitting diode pulses, flow cytometry test beads, and fluorescently labeled cells. The relative signal to noise performance of the APD and PMT was evaluated over the 500 nm to 1050 nm wavelength range using pulsed light emitting diode light sources. While APDs have higher quantum efficiency but lower internal gain than PMTs, with appropriate external amplification the APD has signal to noise response that is comparable to PMTs in the 500 nm to 650 nm range and improved response in the 650 nm to 850 nm range

The data demonstrates that the APD had performance comparable to the PMT in the spectral region between 500 to 650 nm and improved performance in the range of 650 to 1000 nm, where the PMT performance is quite poor. CD4 positive lymphocyte populations were easily identified in normal human blood both by APD and PMT using phycoerythrin labeled antibodies. In contrast, only the APD detector could resolve CD4 positive populations using 800 nm Quantum dot labeled antibodies.

Keywords: APD, avalanche photodiode, flow cytometry, infrared, IR

## 1. INTRODUCTION

The flow cytometer is used to identify cell phenotype and cell function based on light scattering and the emission of fluorescent labels. Specific attributes of individual cells are identified using fluorescent labeled antibodies that bind to receptor sites within the cell or on the cell membrane. The flow cytometer records light scattering and fluorescence intensity of individual cells that are isolated in a hydrodynamically focused flow stream. Current commercial instruments use photomultiplier tubes to detect this emission. Avalanche photodiodes (APDs) are silicon photodetectors that have higher detection efficiency than photomultiplier tubes (PMTs) over the 400 nm to 1100 nm wavelength range. These solid state detectors are smaller than the vacuum tube PMTs. Avalanche photodiodes that are operated with a high voltage bias also have an internal gain mechanism similar to a PMT that produces a large output current for each initial photoelectron. However, to achieve the best signal to noise response, the APD is operated with a lower gain than the PMT. We present a comparison of avalanche photodiodes to photomultiplier tubes that includes the impact of the differences in the detection efficiency, spectral response range, internal gain, and inherent noise sources on the application in flow cytometry.

Early flow cytometry instruments used forward scatter, side scatter, and a single fluorescent marker to identify cells (1). Newer instruments enable detailed identification of cell type and function based on the fluorescence of multiple cell markers (2,3). Each cell marker is labeled with a different dye and emits in a different wavelength range. More labels allow more specification in the identification of the cell. State of the art instruments use multiple lasers and multiple detectors to excite as many as seventeen fluorescent labels (4).

The spectral range that flow cytometry instruments can work in is limited by the excitation source, dye properties and the detector response. Figure 1 illustrates the working wavelength range of excitation sources, dye labels, and the detectors. The bars at the bottom of the figure indicate some of the most common excitation sources including the 488 nm argon ion laser. The excitation wavelength is the high energy limit of the working fluorescence range of the flow cytometer since the Stokes shifted emission is at lower energy than the excitation energy. Organic dyes have limited Stokes shift, so the peak of the emission is typically quite close to the peak of the excitation. While the small energy shift can limit the working wavelength range, tandem dyes have been developed that use Forster energy transfer to shift the emission to longer wavelengths. Quantum dot labels with very large Stokes shifts have also been developed for use in flow cytometry. 488 nm laser sources can efficiently excite the range of quantum dots that will emit across the 500 nm to 800 nm wavelength range. The emission peaks of the Invitrogen quantum dots are shown in Figure 1. Near infrared (NIR) dyes that have an emission peak at wavelengths longer than 800 nm have been developed, however, these dyes require far red excitation sources (5).

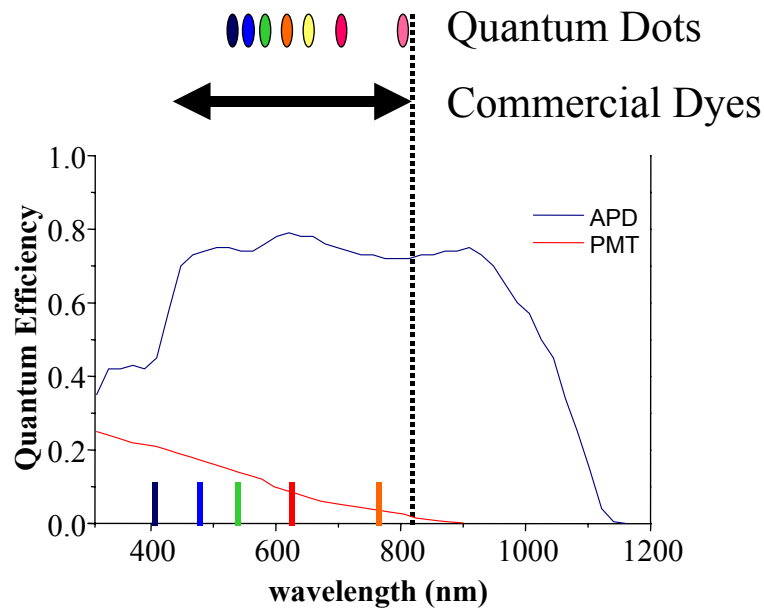


**Figure 1. Quantum efficiency of the APD and PMT detectors.** The bars on the lower axis indicate the typical excitation wavelengths at 405 nm, 488 nm, 532 nm, 632 nm, and 785 nm. The range of emission wavelengths of commercial dyes and the emission peaks of the quantum dots are shown at the top of the figure.

Avalanche photodiodes have high quantum efficiency from 400 nm out to 1100 nm in the near IR (6), and this extended spectral response can be used to extend the operating wavelength range of a flow cytometry system. Figure 1 illustrates the absolute quantum efficiency of the APD and PMT detectors. Since the PMT has limited detection efficiency beyond 800 nm, and there are few dyes available at that wavelength, 800 nm has become the practical long wavelength limit for the flow cytometer operating range. Radiation Monitoring Devices Inc. produces silicon APDs that range in size from 0.5 mm<sup>2</sup> to 4000 mm<sup>2</sup>. (Note: W.L., G.V. and G.E. work at Radiation Monitoring Devices) These detectors are fabricated using a 60 micron thick diffused P-type semiconductor layer on an N type substrate that forms a photosensitive P-N junction at the front of the device. The wavelength response of the detector is defined by the absorption of light in the active region of the device. Long wavelength photons have lower probability of absorption in the active area of the detector and therefore have lower detection efficiency (7).

## 2. EXPERIMENTAL SECTION

We have built a prototype flow cytometer using the optical components of a BD FACScan flow cytometer and the data collection electronics from a BD FACStar flow cytometer (BD Biosciences, San Jose CA.). The samples were excited using a 488 nm argon ion laser with 20 to 40 mW power at the entrance to the sample cell (5500 ASL Ion Laser

Technologies). The beam steering, beam shaping, and focusing optics from the FACScan were used to control the laser beam used to excite the sample. The compound collection lens ( $F=1.2$ ) of the FACScan sample assembly was coupled to the sample flow chamber using index matching grease, and focused the light to a 100 micron pinhole. The pinhole passed the side scatter and fluorescence from the sample and blocked the extraneous laser scatter from the edges of the flow chamber. A 520 nm long wave pass filter separated the 488 nm side scatter from the fluorescence, and a 50 / 50 beamsplitter directed half the emission to an R9220 PMT (Hamamatsu, Hamamatsu City, Japan) and half the emission to an S0223 APD (Radiation Monitoring Devices Inc., Watertown MA). The PMT and APD each received half of the emission intensity in order to directly compare the detectors performance when monitoring the identical sample population. Bandpass filters from other BD Biosciences instruments were used to isolate the relevant emission wavelength ranges. Some of the bandpass filters were partially transmissive at wavelengths longer than 800 nm. This is not an issue with the PMT since the detection efficiency beyond 800 nm is less than one percent. However, the APD is quite sensitive to the longer wavelengths, therefore a 700 nm short pass filter was used with the 530 nm and 585 nm bandpass filters.

In these studies we used a 2mm x 2mm APD detector. The device was used at room temperature with no added temperature stabilization. The APD element was contained in a metal housing without any protective window. A radioactive  $^{55}\text{Fe}$  x-ray source was used to calibrate the response of the APD detector, and a window would block the calibration source. An applied bias between 1550 and 1650 V was used to control the internal gain of the APD. The optimum signal to noise of the APD occurs when the gain is in the range of 200 to 500. This internal gain is significantly less than the internal gain of the PMT. An additional amplifier stage was used with the APD to increase the output signal and make it comparable to the PMT. The amplifier was designed such that the signal would be directly comparable to the PMT and both detectors could be plugged into the same data collection electronics.

Pulsed light emitting diodes, flow cytometry test beads and labeled cells were all used as signal sources in these measurements. Light emitting diodes (LEDs) have been used to quantify the performance of photodetectors for flow cytometry applications. These light sources are very convenient because they provide a reproducible, controlled intensity, wide wavelength variation, and variable time duration. The light output and wavelength can be adjusted to match the output that would be expected from fluorescent labeled cells, yet they do not have the additional noise sources such as laser scatter, autofluorescence, or Raman emission. The LEDs are a simplified surrogate for actual flow cytometry applications. A white Luxeon (Philips Lumileds, San Jose CA) LED was used to provide light over the 500 to 700 nm wavelength range. Twelve red and near infrared LEDs from Roithner Lasertechnik (Wien Austria) were used as signal sources over the 650 nm to 1060 nm range. A pulse generator was used to control the intensity and duration of the pulse emitted by the LED. The LED output was coupled to an optical fiber and directed to a 1/8 meter monochromator (Optometrics Minichrom Ayer MA). The monochromator had a wavelength resolution of 2 nm and the output was coupled to another optical fiber. The end of the fiber was placed at the focus of the cytometer collection optics such that half of the light from the fiber went to the PMT and half went to the APD.

Flow cytometry test beads provided a more realistic signal source for flow instruments. These measurements include other interfering light sources such as laser scatter and Raman emission from the flow sample. These beads can also have weak autofluorescence primarily at longer wavelengths. Flow cytometry test beads with low or mid level intensities are used to optimize PMT gain on commercial instruments(8). We used a six-peak calibration bead set (Spherotech Ultrarainbow URCP-38-2K, Lake Forest, IL), that is packaged in two sample vials. One vial contains calibration test beads with five different levels of dye loading, and another vial contains blank beads with no added dye. This sample is designed to have a broad emission spectrum. The manufacturer supplies calibration data for the relative fluorescent intensity of the beads at different detection wavelengths. The detection wavelengths are defined by bandpass filters, and we used 530 / 30 (530 nm center with 30 nm bandpass), 585 / 42, 690 / 20, 700 nm long wave pass (LWP) and 800 nm LWP.

Samples of white blood cells were obtained from healthy donors and processed on the day they were collected. The whole blood samples were washed once with phosphate buffered saline (PBS) with heparin, and washed again with PBS without heparin. The cells were resuspended in PBS and normal mouse IgG was added to block Fc receptors. One set of samples were incubated with anti-CD4 labeled with phycoerythrin (PE) (clone SK2, BD Biosciences, San Jose CA) in the dark and on ice for 30 minutes. Another set of samples were incubated with anti-CD4 labeled with biotin (Clone S3.5 Invitrogen, Carlsbad CA) using the same method. The monoclonal antibodies and secondary reagents were

used at saturation. Red blood cells were lysed with ammonium chloride (0.15 M NH<sub>4</sub>Cl, 0.5 gm KHCO<sub>3</sub>, 0.1 mM tetra sodium EDTA) and washed with PBS. The CD4 – PE cells were fixed with 2% methanol free formaldehyde (Polysciences, Warrington PA). Cells labeled with CD4-biotin were incubated with QD800 streptavidin conjugated quantum dots (Invitrogen) for 30 minutes and fixed. All of the samples were stored in the dark until use.

### 3. RESULTS

#### 3.1 Pulsed LED source

Light pulses from an LED source provide a convenient surrogate for actual flow cytometry signals that can be used to quantify some aspects of detector performance (9-11). The wavelength, intensity, and pulse duration of the LED output can be controlled to accurately mimic fluorescence emission from labeled cells. The LED pulses have been used to determine the best operating gain that results in the best signal to noise. Figure 2 shows the signal to noise ratio that was measured using 600 nm light pulses with a fixed intensity. The signal to noise ratio was calculated by measuring the mean fluorescence intensity ( $\mu$ ) and the standard deviation ( $\sigma$ ) of the signal histogram. The signal to noise ratio is defined as:

$$\frac{S}{N} = \left( \frac{\mu}{\sigma} \right) = \frac{1}{CV} \quad \text{Eq. 1}$$

which is also the inverse of the coefficient of variation (CV). When the CV is reported in percent the value is multiplied by 100. The signal to noise ratio can be defined more explicitly when the signal is calculated in terms of the incident photon flux and the gain, and the noise is described by the physical processes that create fluctuations in the signal level. These can be written as:

$$\frac{S}{N} = \frac{M\eta\Phi}{\left( M^2 F \eta \Phi + M^2 F \bar{d} + \sigma_{elec}^2 \right)^{1/2}} \quad \text{Eq. 2}$$

where M is the gain,  $\eta$  is the quantum efficiency,  $\Phi$  is the photon flux, F is the excess noise factor, d is the dark noise, and  $\sigma_{elec}^2$  is the variance of the electronic noise (12). The denominator gives a general description of the noise terms for the APD. The first term in the denominator of equation 2 describes the fluctuations in the signal due to shot noise, the second term in the denominator describes the dark noise, and the third term describes the electronic noise. The shot noise and dark noise depend on the excess noise factor F that describes the fluctuations of the internal gain mechanism in APDs and PMTs. The excess noise factor depends on  $k_{eff}$  which is a parameter that describes the relative efficiency of charge amplification of electrons and holes and is given by McIntyre's model (13,14) as:

$$F = k_{eff}M + (2-1/M)(1-k_{eff}) \quad \text{Eq. 3}$$

Previous measurements of similar APD detectors have found  $k_{eff}$  values of  $7 \times 10^{-4}$  (12). For these devices the excess noise varies from 1.8 to 2.4 over the typical operating gains of the device. At high APD gain the excess noise factor is proportional to the gain (15). The excess noise factor also contributes to the noise of the PMT, however the excess noise of the PMT is initially large and approaches one at reasonable working gain.

At low operating gain the excess noise factor is approximately constant, and the fixed electronic noise dominate noise term. Under these conditions the signal to noise increases proportionally with gain. Under high gain operation, the excess noise factor is proportional to the gain and the signal to noise ratio decreases as the square root of the gain. Between the low gain and high gain limits the signal to noise reaches a maximum that is illustrated in Figure 2. This maximum occurs around a gain of 200 to 500. The optimum gain of the APD is substantially lower than the normal operating gain of the PMT. An additional external amplification stage is added to the APD to produce an output that is

similar in amplitude and bandwidth to the PMT output. The APD and external amplifier are designed as a functional replacement for the PMT, and can be plugged into the FACStar data collection console.

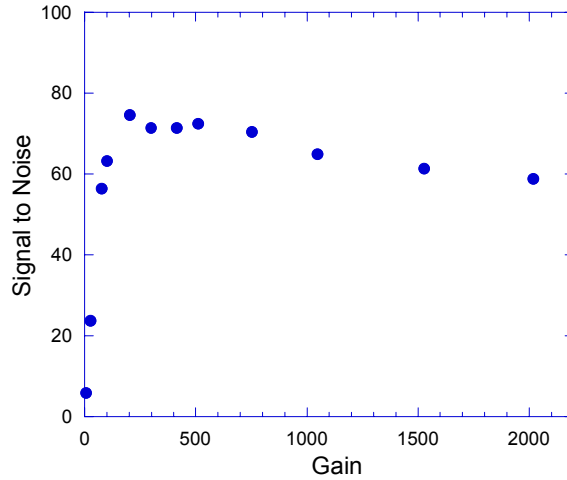


**Figure 2. Signal to noise ratio measured as a function of gain with a constant light intensity at 600 nm.**

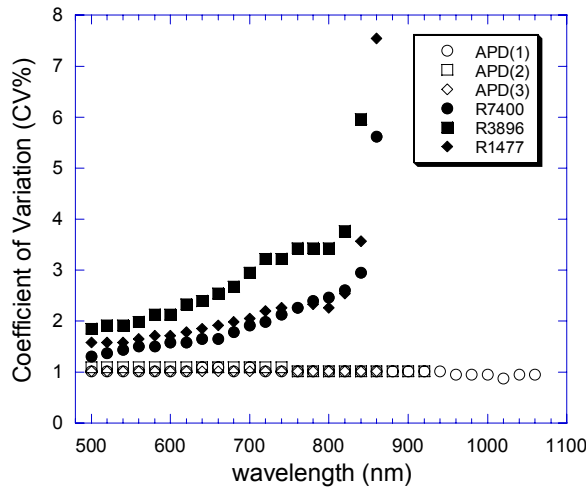


**Figure 3. Coefficient of variation as a function of wavelength for the APD and three PMTs as a function of wavelength at a constant signal level.**

The pulsed LED light source is used to measure the CV of the APD and three different PMTs as a function of wavelength at a fixed signal level, and the results are shown in Figure 3. The signal depends on the gain, quantum efficiency and incident photon flux for each detector, and the quantum efficiency of both detectors changes with

wavelength. The wavelength of the light was selected using the monochromator and directed to the APD and a PMT using a 50 / 50 beamsplitter. The APD is operated with a constant gain of 350, and the signal, which is measured by the mean fluorescence intensity (MFI) was fixed at channel 980 of the output histogram. The mean fluorescence intensity of the APD signal is kept at a constant value of 980 by changing the intensity of the light at each wavelength. The MFI of the PMT is kept constant at each wavelength by increasing the voltage of the detector to match the MFI of the APD. The PMT voltage was lowest at 500 nm and increased at longer wavelengths where the quantum efficiency was lower. When the PMT voltage reached 900 volts, the PMT measurements were stopped. The CV of the APD response was flat by the design of the experiment. The PMT response is presented relative to the flat wavelength dependence of the APD. Because the quantum yield of the PMT is lower at longer wavelengths, fewer initial photoelectrons are generated and the higher gain is required to get the same signal level. The higher gain produces higher noise and higher CV.

### 3.2 Flow cytometry test beads

Flow histograms of a 6-peak flow cytometry calibration test bead set are simultaneously recorded using both the APD and PMT detectors. The test beads are 3.8 micron diameter polystyrene spheres that include blank beads and 5 distinct populations of beads with different fluorescent intensity levels. The beads are available as the Spherotech Ultra Rainbow Calibration set and are designed to be used in the spectral bandpass regions used for flow cytometry measurements over the 400 nm to 800 nm range, however the emission intensity decreases in the red and near infrared.

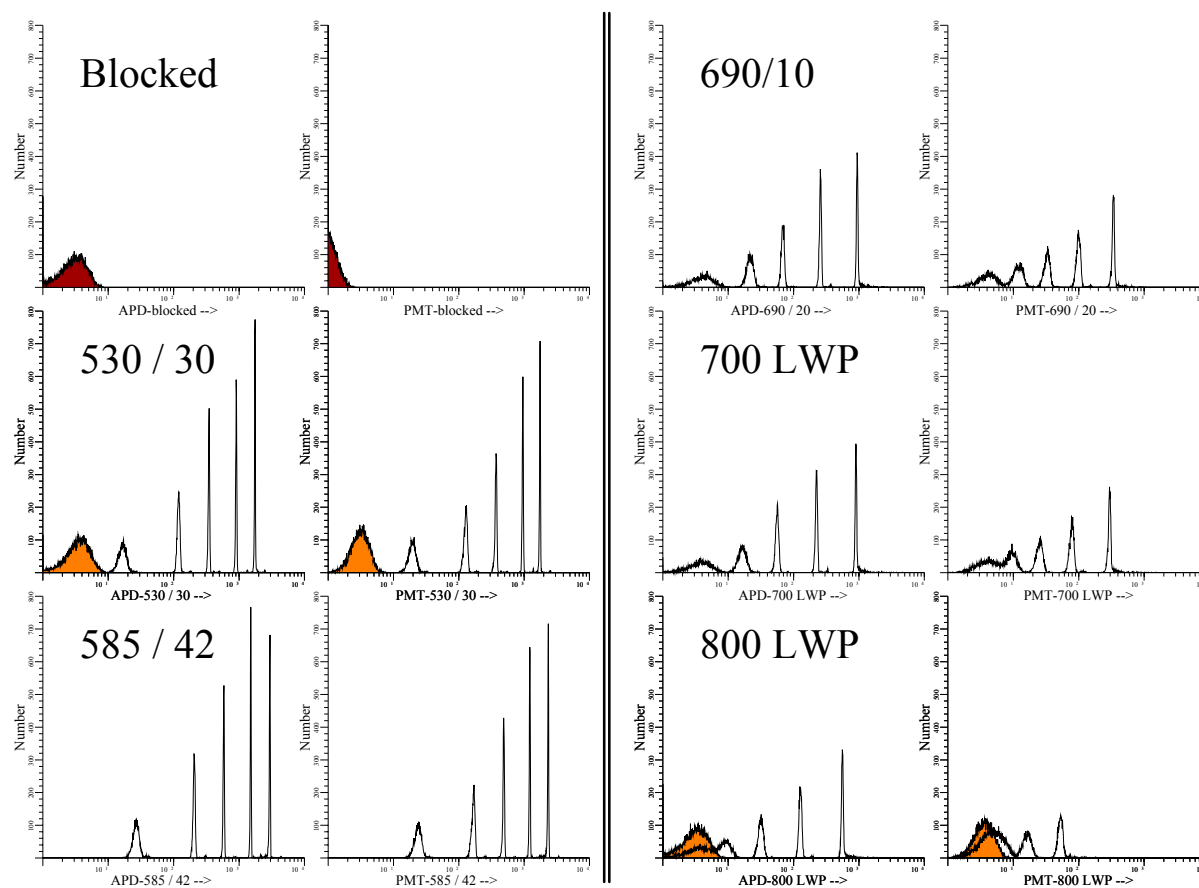


**Figure 4. Flow histograms of the Spherotech Ultra Rainbow Calibration bead set that are recorded simultaneously using the APD and PMT (Hamamatsu R9220) detectors. The histograms are recorded with the detectors blocked, and at five different spectral regions. The filled peaks show the blank bead measurements at 530 / 30 and at 800 LWP.**

Figure 4 shows the histograms of the 6 peak bead set measured simultaneously with the APD and PMT detectors in different spectral bands. The first panel in the upper left shows the noise background measured with the detectors blocked, and triggered by beads flowing in the sample cell. These two plots illustrate the differences between the baseline noise levels that are due to dark noise and electronic noise. This shows that the APD has higher background noise than the PMT and this is primarily attributed to higher thermal dark noise. The following panels show both the APD and PMT measured within a specific spectral bandpass.

The test bead measurements at 530 nm show the peaks for the five dye labeled test beads and the blank bead is shown as the filled peak. The MFI channel of the blank bead peak depends on the dark noise and electronic noise that are shown in the blocked data and also includes other noise sources that are primarily from light sources that are not associated with the fluorescent label emission (11,16). These other photon sources include autofluorescence, laser light scatter, and raman emission from the carrier fluid. When these other sources are included, the negative peak is quite similar for both the APD and PMT. The MFI distribution of the blank beads were also recorded with the 800 nm long wave pass filter and are shown as the solid peaks in the lower left panels of Figure 4. Similar results are expected at the other wavelengths. The gain of both detectors are set such that the signal from the blank beads is within the first decade of the histogram, and the MFI of the brightest bead is the same for the APD and PMT at 530 nm. All of the other measurements in this figure are recorded at the gain established in the measurements at 530 nm.

The histogram of the flow cytometry test beads recorded at 585 nm is shown in Figure 4. The 5 dye labeled beads are measured at the same gain that was used for the 530 nm measurements. In this case the MFIs of the peaks measured with the APD are higher than the PMT since the quantum efficiency of the PMT is lower relative to the quantum efficiency of the APD. This effect is more pronounced for the 690 nm measurements in which the MFI of the peaks measured with the APD are substantially higher than those for the PMT. In addition, the peaks of the PMT are substantially broader than the peaks of the APD and result in larger CVs for the PMT based measurements. The mean fluorescence intensities of the beads measured with the APD are lower at 690 nm than at 585 nm even though the detection efficiency of the APD is very similar at both wavelengths. This indicates that fewer photons are reaching the detector. This occurs because the detection bandpass at 585 nm is 42 nm while the detection bandpass at 690 is only 10 nm. With the lower intensity, the weakest bead fluorescence at 690 nm would not be resolvable from the blanks with either the PMT or APD. Similar results are observed for the 700 nm long wave pass (LWP) measurements in which the weakest peak is within the first decade of the flow histogram and would not be resolved from the blank beads. A dramatic difference is observed between the APD and PMT for the 800 nm LWP measurements that show both the five dye labeled peaks and the blank beads. The APD resolves four of the five dye labeled populations while the dimmest beads are buried beneath the blank bead peak. In contrast only two of the dye labeled bead populations are resolved using the PMT and the other populations have coalesced into a single peak that is not resolved from the blank bead signal. These results show that the APD has similar performance to the PMT detector at 530 and 585 nm spectral ranges and has better performance than the PMT in the near infrared.

Equation 2 shows that the signal to noise and equivalently the CV depend on the signal intensity and the relative contribution of the noise terms. This effect can be demonstrated by measuring the CV of the PMT and APD at different signal intensity levels. Figure 5 illustrates the CV measured for a range of bead fluorescence levels at constant detector gain. In these measurements the APD has a voltage of 1591 Volts and a gain of 350. The PMT voltage is at 490 V to match the APD signal level at 585 nm. Figure 5 shows that the PMT has lower CV at low MFI while the insert to the figure shows that the APD has consistently lower CV at high fluorescence intensity. The total noise at high signal levels is dominated by the shot noise. Since the APD has higher detection efficiency, the relative fluctuations in the detected signal are lower than the PMT. At low fluorescence intensity, the dark noise of the APD is significant compared to the total signal level. The PMT does not have this dark noise contribution and has a lower CV. At low signal intensities the CV of the PMT is lower than the CV observed for the APD, however, there is a crossover point of intensity where the CV of the APD is lower than the PMT. This crossover point is different for all wavelengths and depends on the details of the detection efficiency and noise contributions for each detector.

## Incident Photons

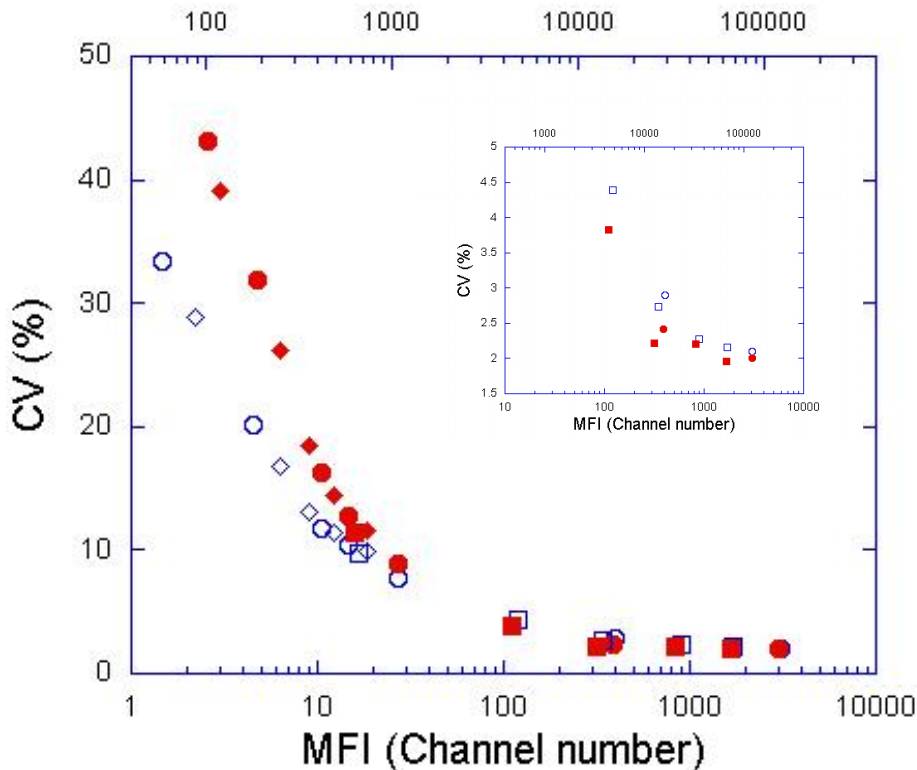


**Figure 5. Coefficient of Variation as a function of the fluorescent intensity measured in the 585 / 42 nm bandpass.**

### 3.3 CD4 labeled cells

The differences between the APD detector and the PMT detector are demonstrated by comparing the identification of CD4 positive cells using CD4 antibodies labeled with phycoerythrin that has an emission maximum at 585 nm, and CD4 antibodies labeled with QD800 quantum dots that have an emission maximum at 800 nm. Figure 5 shows the histograms for the APD and PMT detectors and the forward scatter and side scatter channels that define the detection gate. The gate is set to collect both the lymphocyte and monocyte populations. The top panel of Figure 6 shows the APD and PMT histograms of the unstained cell populations measured with the 585 / 42 bandpass filter. These cells are used to set the gain of the APD and PMT to levels where the signal level from the unstained cells was visible in the first decade of the histogram. The middle panel of Figure 6 shows the CD4-PE labeled cells that were simultaneously detected by the APD and PMT by using the 50 / 50 beamsplitter. The CD4 positive and CD4 dim populations are clearly resolved and distinct from the CD4 negative population for both detectors. The APD voltage was set to 1585 V and operated with a gain of 350. The PMT voltage was set to 475 volts keep the negative peaks in the first decade. The difference between the peak mean fluorescent intensity of the CD4 negative and CD4 positive populations was a factor of 97 for the APD and a factor of 91 for the PMT. These results show comparable performance of the APD and PMT for detection in the 585 / 42 spectral bandpass.

The bottom panel of Figure 6 shows the flow histograms of the QD800 labeled cells recorded with an 800 nm long wave pass filter and the same gain settings used in the middle panel for the detection of PE labeled cells. Under

these conditions the PMT cannot resolve any of the labeled population from the background. The APD can resolve the CD4 positive cells but not the CD4 dim population. The ratio of the peak of the MFI between the CD4 positive and negative population is only a factor of 10 compared to almost 100 for the PE labeled cells. These measurements demonstrate the capability of the APD detector to identify labeled cell populations in the near infrared that cannot be identified using the PMT.

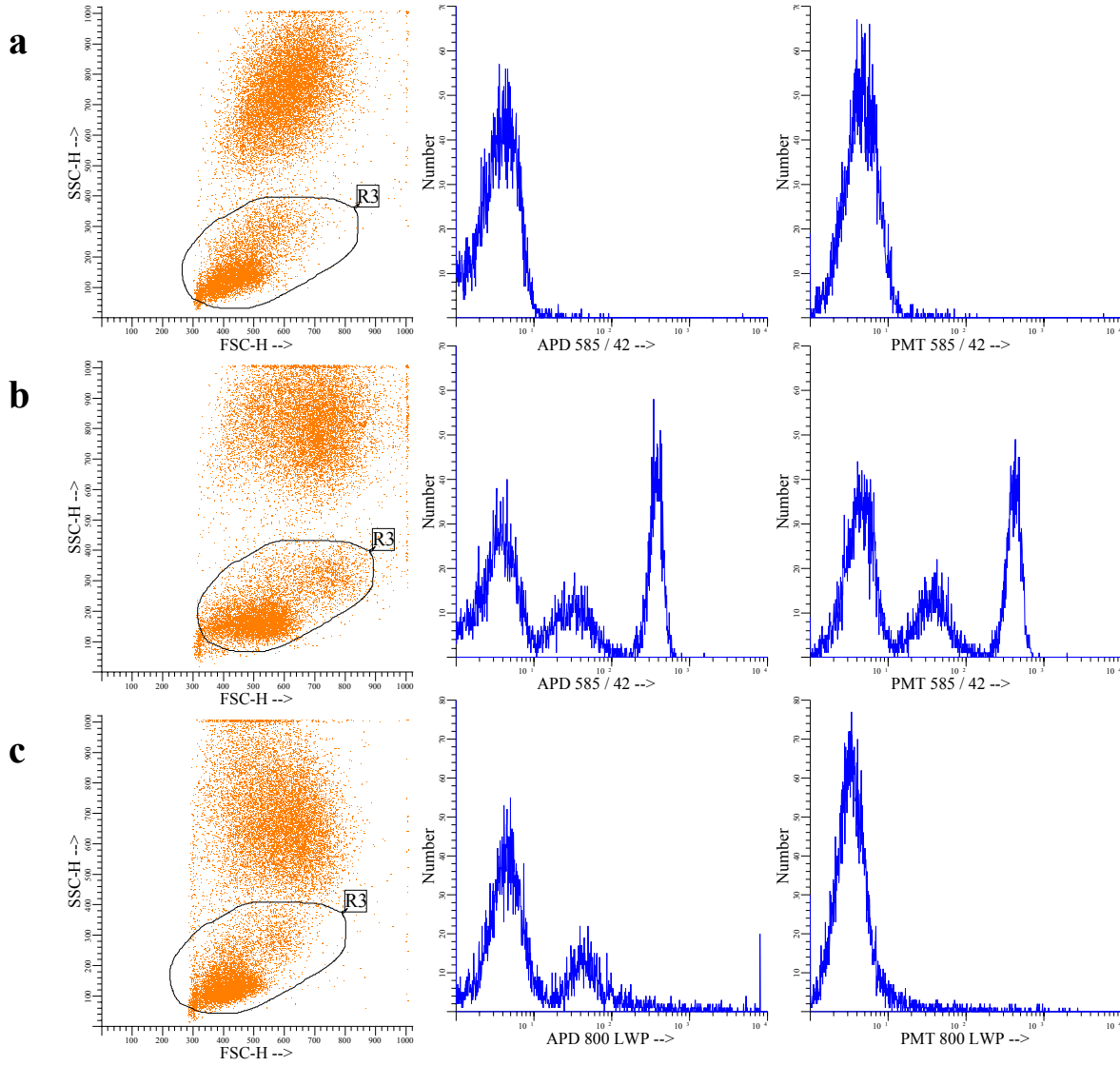


**Figure 6. Flow cytometer histograms of the CD4 positive cells detected simultaneously with the APD and PMT detectors. The top panels show the results for unstained cells detected with the 585 / 42 nm bandpass filter. The middle panels show the phycoerythrin labeled cells detected with the 585 / 42 nm bandpass filter. The bottom panel shows the QD800 labeled cells detected with an 800 nm long wave pass filter**

#### 4. DISCUSSION

The avalanche photodiodes have a number of attributes that make them attractive as detectors for flow cytometry. They have high quantum efficiency and a broad spectral response range that enables sensitive detection of red and near infrared fluorescent labels. The APDs have internal gain that provides low noise amplification of the initial

photon generated signal. Additional external amplification can be used to match the gain and output impedance of the PMT. These detectors are small and can be used to reduce the size of flow instruments.

The most important difference between the PMT and the APD is the impact of the total noise on the detector performance. APD detectors have higher dark noise and higher gain noise than the PMT, but these factors are partially offset by the higher quantum efficiency. The impact of these noise factors can be illustrated by examining the limiting cases of very high intensity signals and very low intensity signals. The signal to noise ratio is an important measure of the detector performance and is defined by equation 2. We can compare the signal to noise ratio at low signal levels for the APD and PMT. The APD has higher dark noise than the PMT and this term dominates the total noise term of the APD. Since the quantum yield of the APD is higher than the PMT, a lower gain,  $M$ , can be used to get the same signal level for a given intensity. However, this does not compensate for the increased dark noise at low signal levels. The impact of the dark noise on the signal to noise ratio and CV at low light levels is demonstrated in Figure 5. The CV of the APD in the first decade at low signal level is higher than the PMT.

At high signal levels, the photon flux,  $\Phi$ , dependent terms dominate the fixed dark noise and electronic noise terms. Equation 2 reduces to a simpler form shown in equation 4, that depends on the quantum efficiency, flux, and the excess noise factor. The excess noise factor of the APD is unity at low gain and increases to 2 under reasonable operating conditions. At very high gain, the excess noise factor scales with the gain. In contrast the excess noise factor of the PMT is large at low gain but rapidly approaches unity under reasonable operating conditions. The total signal to noise depends on both the excess noise and the quantum efficiency. While the excess noise factor of the PMT is a factor of 2 smaller than the APD, the quantum efficiency of the APD can be four or more times larger than the PMT. The signal to noise at high signal intensity is expected to be better for the APD than the PMT, and this effect becomes more pronounced at longer wavelengths when the quantum efficiency of the PMT is low. This effect is illustrated in the insert to figure 5, which shows that the CV's of the APD are consistently lower than the PMT at high signal levels. This effect becomes less important when the intensity fluctuations in the sample are significant as is the case with most biological samples. The CVs of both the APD and PMT converge to a limiting value at high intensity, and this is a result of the intensity distribution of the sample beads used for Figure 5.

$$\frac{S}{N} = \left( \frac{\eta\Phi}{F} \right)^{1/2} \quad \text{Eq. 4}$$

## 5. CONCLUSION

These measurements demonstrate the use of the APD detector for flow cytometry by measuring flow test particle samples and identifying CD4 positive cell populations. The flow cytometry test beads are used to demonstrate the relative performance of the APD and PMT detectors at different intensities and wavelengths. These studies show that in the visible wavelength region, the APD has comparable performance to the PMT at most signal levels, while the PMT has better signal to noise performance only at low signal levels. In the red and near infrared spectral regions, the APD has better signal to noise performance than the PMT at low and high signal intensity conditions. The identification of CD4 positive cells in human blood is used to demonstrate that the APD and PMT have similar performance when using phycoerythrin as the fluorescent label, but only the APD can identify the CD4 positive cells when using the 800 nm quantum dots as the fluorescent label.

1. Bonner WA, Hulett HR, Sweet RG, Herzenberg LA. Fluorescence Activated Cell Sorting. *Rev. Sci. Instrum.* 1972;43:404-409.
2. Roederer M, DeRosa S, Gerstein R, Anderson M, Bigos M, Stovel R, Naozaki T, Herzenberg L, Herzenberg L. 8 Color, 10-Parameter Flow Cytometry to Elucidate Complex Leukocyte Heterogeneity. *Cytometry* 1997;29:328-339.

3. DeRosa S, Herzenberg L, Herzenberg L, Roederer M. 11-color, 13-parameter flow cytometry: Identification of human naive T cells by phenotype, function and T-cell receptor diversity. *Nature Medicine* 2001;7(2):245.
4. Perfetto SP, Chattopadhyay PK, Roederer M. Seventeen-colour flow cytometry: unravelling the immune system. *Nature* 2004;4:648-655.
5. Stewart CC, Woodring ML, Podniesinski E, Gray B. Flow Cytometry in the Infrared: Inexpensive Modifications to a Commercial Instrument. *Cytometry Part A* 2005;67A:104-111.
6. Farrell R, Redus, R., Gordon, J. S., Gothoskar, P., High Gain APD Array for Photon Detection. *Proceedings SPIE* 1995.;2550:266.
7. McClish M, Farrell R, Vanderpuye K, Shah KS. A Reexamination of Deep Diffused Silicon Avalanche Photodiode Gain and Quantum Efficiency. *IEEE Transactions on Nuclear Science* 2006;53(5):3049.
8. Sasaki DT, Maecker H, Trotter J. Establishing Optimum Baseline PMT Gains to Maximize Resolution on BD Biosciences Digital Flow Cytometers; 2005.
9. Chase ES, Hoffman RA. Resolution of Dimly Fluorescent Particles: A Practical Measure of Fluorescence Sensitivity. *Cytometry* 1998;33:267-279.
10. Steen HD. Noise, Sensitivity and Resolution of Flow Cytometers. *Cytometry* 1992;13:822-830.
11. Pinkel D, Steen HD. Simple Methods to Determine and Compare the Sensitivity of Flow Cytometers. *Cytometry* 1982;3(3):220-223.
12. Redus R, Farrell R. Gain and noise in very high gain avalanche photodiodes: theory and experiment. In: Hoover R, Doty P, editors; 1996. *SPIE*. p 288-297.
13. McIntyre RJ. Multiplication noise in uniform avalanche photodiodes. *IEEE Transactions on Electron Devices* 1966;ED-13:164-168.
14. Webb PP, McIntyre RJ, Conradi J. Properties of Avalanche Photodiodes. *RCA Review* 1974;35:234.
15. Teich MC, Matsuo K, Saleh BEA. Excess Noise Factors for Conventional and Superlattice Avalanche Photodiodes and Photomultiplier Tubes. *IEEE Journal of Quantum Electronics* 1986;QE-22(8):1184.
16. Ubezio P, Andreoni A. Linearity and Noise Sources in Flow Cytometry. *Cytometry* 1985;6:109-115.